124.0 (s, C_5Me_5), 96.9 (t, J = 122 Hz, TaCHCHCH$_2$CH$_2$), 44.2 (t, J = 125 Hz, TaCHCHCH$_2$), 12.3 (q, J = 128 Hz, C_5Me_5).

Collection of the X-ray Diffraction Data for Ta(η^5-C_5Me_5)($C_6H_5C{\equiv}CC_6H_5$)Cl_2. A well-formed orange parallelepiped of approximate dimensions 0.20 × 0.20 × 0.19 mm was carefully wedged into a 0.2-mm diameter thin-walled capillary, which was then purged with argon, flame-sealed, fixed into an aluminum pin with beeswax, and mounted into a eucentric goniometer.

The crystal was aligned and data were collected on our Syntex $P2_1$ automated diffractometer with use of methods described previously.[11] Crystal parameters can be found in Table VII.

Solution and Refinement of the Structure. The structure was solved by using the Syntex XTL system on our in-house NOVA 1200 computer. Scattering factors for neutral atoms were used in their analytical forms;[12a] the contributions of all nonhydrogen atoms were corrected for both the real ($\Delta f'$) and imaginary ($\Delta f''$) components of anomalous dispersion.[12b] The function minimized in the least-squares refinement process was $\sum w(|F_o| - |F_c|)^2$; the weights used (w) were derived from the stochastic $\sigma(|F_o|)$ values, modified by an ignorance factor (p) of 0.015 (see eq 5).

$$w = [(\sigma(|F_o|))^2 + (p|F_o|)^2]^{-1} \quad (5)$$

A Patterson synthesis was used to locate the tantalum atom. A series of difference-Fourier syntheses, each being phased by an increasing number of atoms, yielded all 26 remaining nonhydrogen atoms. Hydrogen atoms of the $C_6H_5C{\equiv}CC_6H_5$ ligand were included in calculated positions, based upon d(C–H) = 0.95 Å,[13] and were updated as necessary. Full-matrix least-squares refinement led to final convergence with R_F = 3.3%, R_{wF} = 3.1%, and GOF = 1.346 for all 2884 independent reflections (*none* rejected) with 244 variables. The discrepancy indices for those 2571 reflections with $I > 3\sigma(I)$ were R_F = 2.6% and R_{wF} = 3.0%.

A final difference-Fourier synthesis was devoid of significant features. (The highest peak was of height 0.56 e Å^{-3}, and there were indications of the positions of some, *but not all*, hydrogen atoms associated with the η^5-C_5Me_5 ligand; this aspect was not further pursued.)

The unsual tests of the residual, $\sum w(|F_o| - |F_c|)^2$, vs. $|F_o|$, $(\sin\theta)/\lambda$, sequence number, and identity or parity of the Miller indices, suggested that the weighting scheme was satisfactory. Final positional and thermal parameters are collected in Tables II and III.

Acknowledgment. This work was supported by the National Science Foundation (Grants CHE79-24560 to M.R.C. and CHE79-05307 to R.R.S.).

Registry No. Ta(η^5-C_5Me_5)(PhC≡CPh)Cl_2, 75522-28-0; Ta(η^5-C_5Me_5)(PhC≡CPh)(OMe)Cl, 75522-29-1; Ta(η^5-C_5Me_5)(PhC≡CPh)$(OMe)_2$, 75522-30-4; Ta(η^5-C_5Me_5)(MeC≡CMe)Cl_2, 75522-31-5; Ta(η^5-C_5Me_5)(EtC≡CEt)Cl_2, 75522-32-6; Ta(η^5-C_5Me_5)(PhC≡CH)Cl_2, 75522-33-7; Ta(η^5-C_5Me_5)(EtC≡CEt)Br_2, 75522-34-8; Ta(η^5-C_5Me_5)(HC≡CH)Cl_2, 75522-35-9; (η^5-C_5Me_5)Cl_2TaCHCHCH$_2$CH$_2$, 75522-36-0; Ta(η^5-C_5Me_5)(styrene)Cl_2, 71414-50-1; Ta(η^5-C_5Me_5)(cyclooctene)Cl_2, 71414-52-3; ethylene, 74-85-1; Ta(η^5-C_5Me_5)(cyclooctene)Br_2, 74594-03-9.

Supplementary Material Available: A listing of observed and calculated structure factor amplitudes (13 pages). Ordering information is given on any current masthead page.

(11) Churchill, M. R.; Lashewycz, R. A.; Rotella, F. J. *Inorg. Chem.* **1977**, *16*, 265–271.
(12) "International Tables for X-Ray Crystallography"; Kynoch Press: Birmingham, England, 1974; Vol. IV: (a) pp 99–101; (b) pp 149–150.
(13) Churchill, M. R. *Inorg. Chem.* **1973**, *12*, 1213–1214.

Contribution from the Istituto di Chimica Generale ed Inorganica dell'Università, Laboratorio CNR, 50132 Firenze, Italy, and the Istituto di Chimica Generale ed Inorganica della Facoltà di Farmacia, 50121 Firenze, Italy

ESR Spectra of Cobalt(II)- and Copper(II)-Doped Bis(*N*,*N*-bis(2-(diethylamino)ethyl)((2-hydroxyethyl)amino-*O*)dinickel(II) Diperchlorate. Characterization of Nickel(II)–Cobalt(II) and Nickel(II)–Copper(II) Exchange-Coupled Pairs

LUCIA BANCI, ALESSANDRO BENCINI, ANDREA DEI,[1] and DANTE GATTESCHI*

Received December 6, 1979

The ESR spectra of cobalt(II)- and copper(II)-doped bis(*N*,*N*-bis(2-(diethylamino)ethyl)((2-hydroxyethyl)amino-*O*)dinickel(II) diperchlorate ($[Ni_2(bdhe)_2](ClO_4)_2$) have shown the presence of nickel(II)–cobalt(II) and nickel(II)–copper(II) pairs. For comparison purposes also the ESR spectra of copper(II)-doped zinc(II) analogue have been recorded. The g values of the pairs have been related to the g values of the individual ions through a vector coupling relation which has been tested with use of available literature data. The effect of large zero field splittings of the individual ions has been discussed. The sign of the interaction has been shown to be antiferromagnetic for the nickel(II)–copper(II) pair, while no safe conclusion was reached for the nickel(II)–cobalt(II) couple.

Introduction

The spectroscopic and magnetic properties of mixed-transition-metal complexes are attracting increasing interest,[1-7] since they can largely expand the number of experimental data on exchange interactions and give new information to correlate the magnetic properties with the structural features of the complexes.

In general it may be difficult to obtain discrete complexes containing pairs of different metal ions, but it is easier to obtain measurable concentrations of such pairs in the lattices of dinuclear complexes by preparing the compounds starting from variable amounts of two parent metal complexes. Magnetic resonance spectroscopy can then be used in order to reveal the presence of heterodinuclear complexes.[8,9]

* To whom correspondence should be addressed at the Istituto di Chimica Generale ed Inorganica dell'Università.

(1) McPherson, G. L.; Varga, G. A.; Nodine, M. H. *Inorg. Chem.* **1979**, *18*, 2189.
(2) Kahn, O.; Tola, P.; Galy, J.; Coudanne, H. *J. Am. Chem. Soc.* **1978**, *100*, 3931.
(3) Casellato, U.; Vigato, P. A.; Vidali, M. *Coord. Chem. Rev.* **1977**, *23*, 31.
(4) O'Connor, C. J.; Freyberg, D. P.; Sinn, E. *Inorg. Chem.* **1979**, *18*, 1077.
(5) O'Bryan, N. B.; Maier, T. O.; Paul, I. C.; Drago, R. S. *J. Am. Chem. Soc.* **1973**, *95*, 6640.
(6) Kokoszka, G. F.; Duerst, R. W. *Coord. Chem. Rev.* **1970**, *5*, 209.
(7) Kuszaj, J. M.; Tomlonovic, B.; Murtha, D. P.; Lintvetd, R. L.; Glick, M. D. *Inorg. Chem.* **1973**, *12*, 1297. Lintvetd, R. L.; Borer, L. L.; Murtha, D. P.; Kuszaj, J. M.; Glick, M. D. *Ibid.* **1974**, *13*, 18.
(8) Dei, A.; Gatteschi, D.; Piergentili, E. *Inorg. Chem.* **1979**, *18*, 89.

0020-1669/81/1320-0393$01.00/0

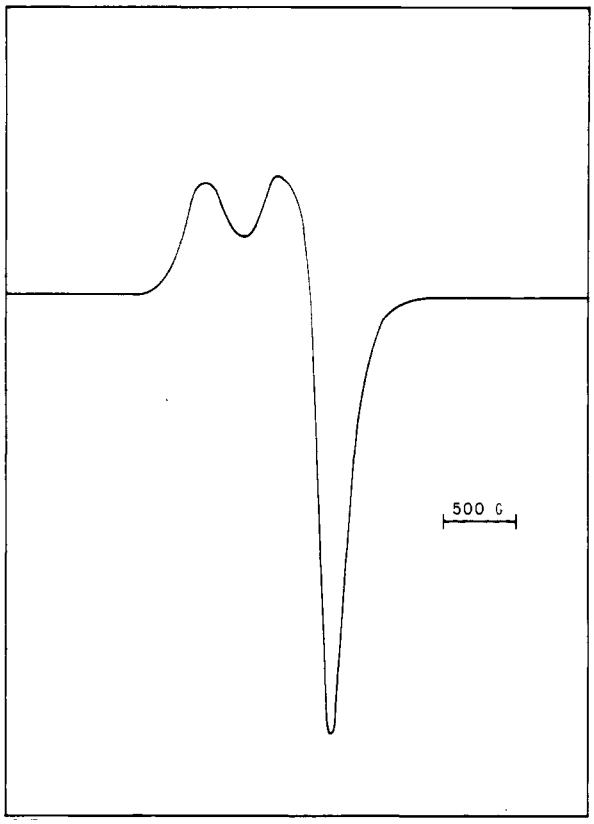

Figure 1. Polycrystalline powder ESR spectrum (9 GHz) of Cu-doped $[Ni_2(bdhe)_2](ClO_4)_2$ at 4.2 K.

In the solid state, ESR spectroscopy can be used to obtain the spin Hamiltonian parameters of the exchange-coupled pairs. Their interpretation, however, may be difficult. In general the g values of the dimer have been related to the g values of the individual ions.[10,11] Although the method can be fruitful in the case of small zero field splitting,[12] we want to show that, when this condition does not hold, the analysis may become unsuccessful. Such effects are shown by the ESR spectra of cobalt(II)–nickel(II) and copper(II)–nickel(II) exchange-coupled pairs observed in the lattice of bis(*N*,*N*-bis(2-(diethylamino)ethyl)((2-hydroxyethyl)amino-*O*))dinickel(II) diperchlorate ($[Ni_2(bdhe)_2](ClO_4)_2$).

Experimental Section

Cobalt(II)- and copper(II)-doped $[M_2(bdhe)_2](ClO_4)_2$ (M = Ni, Zn) derivatives were prepared as described elsewhere.[13] Single crystals suitable for ESR spectra were obtained by slow evaporation of dichloromethane–acetone solutions of the above complexes and oriented on a Perspex rod with the aid of a polarizing microscope.

The crystals of the nickel(II) derivatives were found to conform to the reported structure[14] by the Weissenberg technique, and the crystal faces were identified by the same technique.

Single-crystal ESR and ligand field spectra down to 4.2 K were recorded with the apparatus described elsewhere.[15,16]

Results

The preparation of the $[M_2(bdhe)_2](ClO_4)_2$ complexes has been described elsewhere.[13] If in the reaction mixture both M and M′ perchlorate salts (M, M′ = Co, Ni, Cu, Zn) are added in variable amounts, polycrystalline powders containing M–M and M–M′ dimers can be obtained. Although no analytical support of the existence of M–M′ couples can be achieved, the ESR spectra to be described below give a clear evidence of their presence.

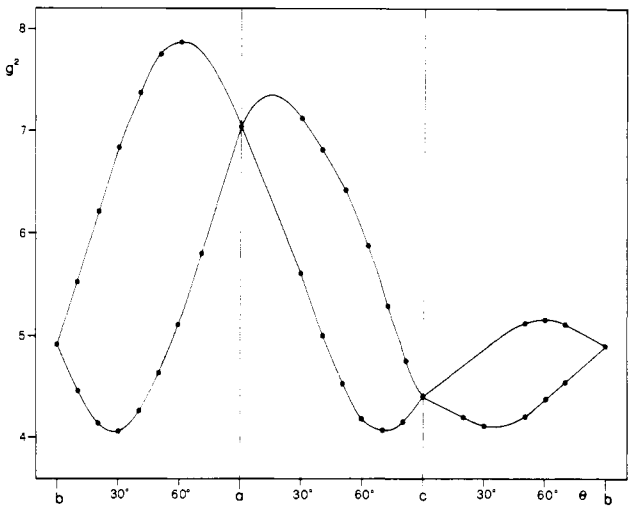

Figure 2. Angular dependence of the g^2 values of Cu-doped $[Ni_2(bdhe)_2](ClO_4)_2$ in the three principal crystal planes.

Table I. Principal g Values and Directions for $[(Ni,Cu)_2(bdhe)_2](ClO_4)_2$[a]

	g		
	2.80	2.03	2.02
l_a	0.85	−0.52	−0.02
l_b	0.45	0.72	0.53
l_c	−0.27	−0.46	0.84

[a] The direction cosines are referred to the crystal axes.

Table II. Direction Cosines of the Relevant Bond Directions in $[Ni_2(bdhe)_2](ClO_4)_2$[a]

	Ni–O(5)	Ni–N(1)	Ni–N(2)	Ni–N(3)	Ni–O(5′)	Ni–Ni′
l_a	−0.3556	−0.8676	−0.2683	0.4206	0.7624	0.2601
l_b	0.6417	−0.4749	0.0089	−0.8684	0.6335	0.8147
l_c	0.6795	0.1473	−0.9633	0.2626	0.1318	0.5182

[a] The direction cosines are referred to the crystal axes.

Since the X-ray crystal structure of the nickel(II) derivative is available,[14] crystals of this compound containing both cobalt(II) and copper(II) in low concentrations were grown. As suggested by variable-temperature susceptibility data,[13] at very low temperature the nickel(II) lattice must be essentially diamagnetic so that it is well suited for ESR experiments. In the following we will use the shorthand notation Ni–M to indicate the samples in which low concentrations of the metal M are present in the nickel lattice.

The polycrystalline powder spectrum of the Ni–Cu sample recorded at liquid-helium temperature is shown in Figure 1. It can be interpreted by using a $S = {}^1/_2$ spin Hamiltonian, yielding $g_{\parallel} = 2.75$ and $g_{\perp} = 2.02$. The signal can be observed only close to 4.2 K.

Single-crystal spectra were recorded with the static magnetic field in the three principal planes of the orthorhombic cell. The spectra confirmed that the observed transitions occur within one Kramers doublet. The angular dependence of the g^2 tensor is shown in Figure 2. The method by Schonland[17] was used in order to obtain the principal g values and directions. Two sets of such values are compatible with the orthorhombic cell,[18]

(9) Banci, L.; Bencini, A.; Dei, A.; Gatteschi, D. *Inorg. Chim. Acta* **1979**, *36*, L419.
(10) Gibson, J. F.; Hall, D. O.; Thornley, J. M. H.; Whately, F. R.; "Magnetic Resonance in Biological Systems"; Ehrenberg, A., Malmstrom, B., Vänngard, T., Eds.; Pergamon Press: New York.
(11) Owen, J. *J. Appl. Phys.* **1961**, *32*, 2135.
(12) Owen, J.; Harris, E. A. In "Electron Paramagnetic Resonance"; Geschwind, S., Ed.; Plenum Press: New York, London, 1972.
(13) Banci, L.; Dei, A. *Inorg. Chim. Acta* **1980**, *39*, 37.
(14) Dapporto, P.; Sacconi, L. *J. Chem. Soc. A* **1970**, 681.
(15) Bencini, A.; Gatteschi, D. *Inorg. Chem.* **1977**, *16*, 2141.
(16) Bertini, I.; Gatteschi, D.; Scozzafava, A. *Inorg. Chem.* **1976**, *15*, 203. Bencini, A.; Benelli, C.; Gatteschi, D. *Ibid.* **1978**, *17*, 3313.
(17) Schonland, D. S. *Proc. Phys. Soc., London* **1959**, *73*, 788.

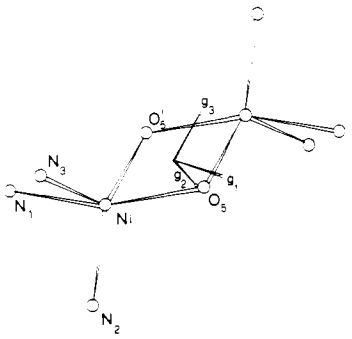

Figure 3. Orientation of the **g** tensor in the molecular frame for Cu-doped $[Ni_2(bdhe)_2](ClO_4)_2$.

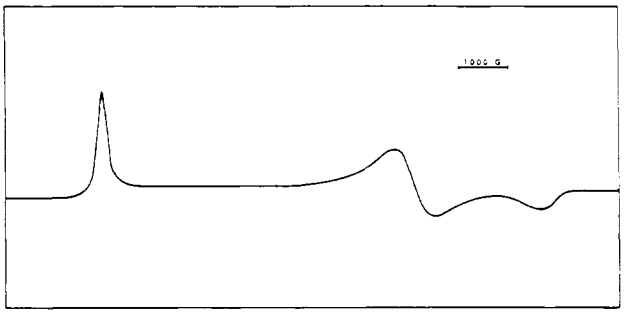

Figure 4. Polycrystalline powder ESR spectrum (9 GHz) of Co-doped $[Ni_2(bdhe)_2](ClO_4)_2$ at 4.2 K.

but one set was rejected since the values did not correspond to those observed in the powder spectra. The principal g values, together with the principal directions are shown in Table I. The orthorhombic symmetry of the cell determines the presence of four magnetically nonequivalent sites. The principal directions of the other three sites can be obtained from those shown in Table I by using the following relations for the direction cosines: $\bar{l}, m, n$; $l, \bar{m}, n$; $l, m, \bar{n}$. In principle each of these sets can be attributed to each molecule in the unit cell. However, according to one choice, the $g_{\parallel}$ value is reasonably close to the bond directions which would individuate the trigonal axis, in the ideal case of two perfect trigonal bipyramids. If the direction cosines of the bond directions shown in Table II are used, the angle made by $g_{\parallel}$ with Ni–O(5′) and Ni–N(1) are calculated to be 26 and 7°, respectively. Figure 3 shows the orientation of the **g** axes in the molecular frame according to this choice.

The polycrystalline powder spectrum of the Ni–Co sample recorded at 4.2 K is shown in Figure 4. Also in this case an $S = {}^1/_2$ spin Hamiltonian seems to be appropriate, yielding $g_1 = 3.4$, $g_2 = 0.8$, and $g_3 = 0.6$. The single-crystal spectra confirmed that the features seen in the powder spectra are associated with one transition. The angular dependence of the g^2 values is shown in Figure 5, and the principal g values and directions are given in Table III. According to one choice, the highest g value is close to the metal–metal direction, making an angle of 14° with it. Figure 6 shows the orientations of the **g** axes in the molecular frame.

For information on the g values of the copper(II) complex, also the polycrystalline powder spectrum of Zn–Cu samples was obtained at Q-band frequency and is shown in Figure 7. The spectra are typical of five-coordinate copper(II) complexes,[18,19] close to the trigonal-bipyramidal limit.[20-22] The spin Hamiltonian parameters are $g_1 = 2.25$, $g_2 = 2.16$, $g_3 = 2.02$, $A_1 = 105 \times 10^{-4}$ cm^{-1}, $A_2 = 50 \times 10^{-4}$ cm^{-1}, and $A_3 = 60 \times 10^{-4}$ cm^{-1}.

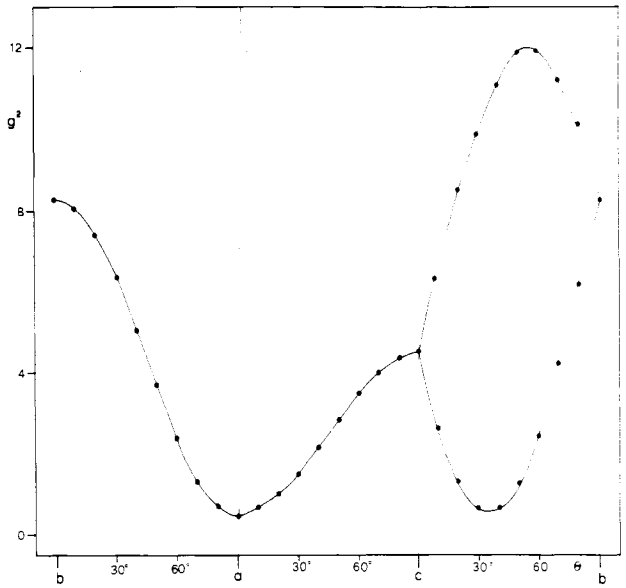

Figure 5. Angular dependence of the g^2 values of Co-doped $[Ni_2(bdhe)_2](ClO_4)_2$ in the three principal crystal planes.

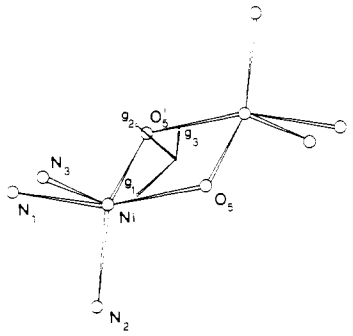

Figure 6. Orientation of the **g** tensor in the molecular frame for Co-doped $[Ni_2(bdhe)_2](ClO_4)_2$.

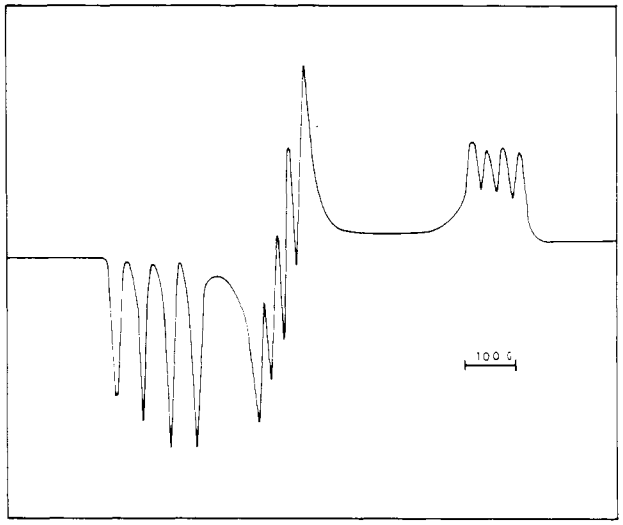

Figure 7. Polycrystalline powder ESR spectrum (35 GHz) of Cu-doped $[Zn_2(bdhe)_2](ClO_4)_2$ at 4.2 K.

Since the structure of the zinc(II) lattice is now known, no single-crystal spectra were recorded. However the comparison with previous literature data suggests that the g_3 must be close to the trigonal axis of the bipyramid.

The single-crystal polarized electronic spectra of the pure nickel(II) complex were recorded to obtain information on the

(18) Bencini, A.; Gatteschi, D. *Transition Met. Chem.*, in press.
(19) Bencini, A.; Bertini, I.; Gatteschi, D.; Scozzafava, A. *Inorg. Chem.* **1978**, *17*, 3194.
(20) Hathaway, B. J.; Billing, D. E. *Coord. Chem. Rev.* **1970**, *5*, 147.
(21) Barbucci, R.; Bencini, A.; Gatteschi, D. *Inorg. Chem.* **1977**, *16*, 2117.
(22) Bencini, A.; Gatteschi, D. *Inorg. Chem.* **1977**, *16*, 1994.

Table III. Principal g Values and Directions for $[(Ni,Co)_2(bdhe)_2](ClO_4)_2$[a]

	g		
	3.47	0.77	0.66
l_a	−0.01	−0.61	0.79
l_b	−0.81	−0.46	−0.37
l_c	−0.59	0.64	0.49

[a] The direction cosines are referred to the crystal axes.

Table IV. Assignment of the Electronic Spectra of $[Ni_2(bdhe)_2](ClO_4)_2$ to the d–d Transitions

abs max, $cm^{-1} \times 10^{-3}$	transition	abs max, $cm^{-1} \times 10^{-3}$	transition
7	$^3E' \rightarrow {}^3E''$	15.2	$^3E' \rightarrow {}^3A_2'$
9		21.2	$^3E' \rightarrow {}^3E''(P)$
11.3	$^3E' \rightarrow {}^3A_1'', {}^3A_2''$	24	$^3E' \rightarrow {}^3A_2'(P)$
12.0			

Table V. Hamiltonian Matrix for a $S_1 = 1, S = {}^1/_2$ Pair[a]

	$\vert{}^3/_2\ \ {}^3/_2\rangle$	$\vert{}^3/_2\ \ {}^1/_2\rangle$	$\vert{}^3/_2\ \ -{}^1/_2\rangle$	$\vert{}^3/_2\ \ -{}^3/_2\rangle$	$\vert{}^1/_2\ \ {}^1/_2\rangle$	$\vert{}^1/_2\ \ -{}^1/_2\rangle$
$\langle{}^3/_2\ \ {}^3/_2\vert$	$(3/2)\mu_B B_z g_z^{3/2} + D_c + J/2$	$(3^{1/2}/2)\mu_B(B_x g_x^{3/2} - iB_y g_y^{3/2})$	$(1/3^{1/2})E_1 + 3^{1/2}E_e$	0	$(1/6^{1/2})\mu_B[(g_{x_1}B_x - ig_{y_1}B_y) - (g_{x_2}B_x - ig_{y_2}B_y)] - (6^{1/2}/4)(d_y + id_x)$	$(2^{1/2}/3^{1/2})E_1 - (1/6^{1/2})E_e$
$\langle{}^3/_2\ \ {}^1/_2\vert$	$(3^{1/2}/2)\mu_B(B_x g_x^{3/2} + iB_y g_y^{3/2})$	$(1/2)(\mu_B B_z g_z^{3/2} + J) - D_c$	$\mu_B(B_x g_x^{3/2} - iB_y g_y^{3/2})$	$(1/3^{1/2})E_1 + 3^{1/2}E_e$	$-(2^{1/2}/3)\mu_B(g_{z_1} - g_{z_2})B_z + (i/2^{1/2})d_z - (2^{1/2}/3)D_1 + [1/(3(2^{1/2}))]D_e$	$(2^{1/2}/6)\mu_B[(g_{x_1}B_x - ig_{y_1}B_y) - (g_{x_2}B_x - ig_{y_2}B_y)] - (2^{1/2}/4)(id_x + d_y)$
$\langle{}^3/_2\ -{}^1/_2\vert$	$(1/3^{1/2})E_1 + 3^{1/2}E_e$	$\mu_B(B_x g_x^{3/2} + iB_y g_y^{3/2})$	$-(1/2)\mu_B B_z g_z^{3/2} + J/2 - D_c$	$(3^{1/2}/2)\mu_B(B_x g_x^{3/2} - iB_y g_y^{3/2})$	$-(2^{1/2}/6)\mu_B[(g_{x_1}B_x + ig_{y_1}B_y) - (g_{x_2}B_x + ig_{y_2}B_y)] + (2^{1/2}/4)(id_x - d_y)$	$-(2^{1/2}/3)\mu_B(g_{z_1} - g_{z_2})B_z + (i(2^{1/2})/2)d_z + (2^{1/2}/3)D_1 - [1/(3(2^{1/2}))]D_e$
$\langle{}^3/_2\ -{}^3/_2\vert$	0	$(1/3^{1/2})E_1 + 3^{1/2}E_e$	$(3^{1/2}/2)\mu_B(B_x g_x^{3/2} + iB_y g_y^{3/2})$	$-(3/2)\mu_B B_z g_z^{3/2} + J/2 + D_c$	$-(2^{1/2}/3^{1/2})E_1 + (1/6^{1/2})E_e$	$-(1/6^{1/2})\mu_B[(g_{x_1}B_x + ig_{y_1}B_y) - (g_{x_2}B_x + ig_{y_2}B_y)] + [3/(2(6^{1/2}))](id_x - d_y)$
$\langle{}^1/_2\ \ {}^1/_2\vert$	$(1/6^{1/2})\mu_B[(g_{x_1}B_x + ig_{y_1}B_y) - (g_{x_2}B_x + ig_{y_2}B_y)] + (6^{1/2}/4)(id_x - d_y)$	$-(2^{1/2}/3)\mu_B(g_{z_1} - g_{z_2})B_z - (i/2^{1/2})d_z - (2^{1/2}/3)D_1 - [1/(3(2^{1/2}))]D_e$	$(2^{1/2}/6)\mu_B[(g_{x_1}B_x - ig_{y_1}B_y) + (g_{x_2}B_x - ig_{y_2}B_y)] - (2^{1/2}/4)(id_x + d_y)$	$-(2^{1/2}/3^{1/2})E_1 - (1/6^{1/2})E_e$	$(1/2)\mu_B B g_z^{1/2} - J$	$(1/2)\mu_B(g_x^{1/2}B_x - ig_y^{1/2}B_y)$
$\langle{}^1/_2\ -{}^1/_2\vert$	$(2^{1/2}/3^{1/2})E_1 + (1/6^{1/2})E_e$	$(2^{1/2}/6)\mu_B[(g_{x_1}B_x + ig_{y_1}B_y) - (g_{x_2}B_x + ig_{y_2}g_y)] - (2^{1/2}/4)(d_y - id_x)$	$-(2^{1/2}/3)\mu_B(g_{z_1} - g_{z_2})B_{z_2} - (i/2^{1/2})d_z + (2/3)D_1 + [1/(3(2^{1/2}))]D_e$	$-(1/6^{1/2})\mu_B[(g_{x_1}B_x - ig_{y_1}B_y) - (g_{x_2}B_x - ig_{y_2}B_y)] - (6^{1/2}/4)(d_y + id_x)$	$(1/2)\mu_B(g_x^{1/2}B_x + ig_y^{1/2}B_y)$	$-(1/2)\mu_B B g_z^{1/2} - J$

[a] The Hamiltonian operator is defined in the text. The axes of g, D_1, D, and d have been considered to be collinear. $g^{3/2} = {}^2/_3 g_1 + {}^1/_3 g_2$; $g^{1/2} = {}^2/_3 g_1 - {}^1/_3 g_2$; $D_c = D_e/3 + D_1/3$.

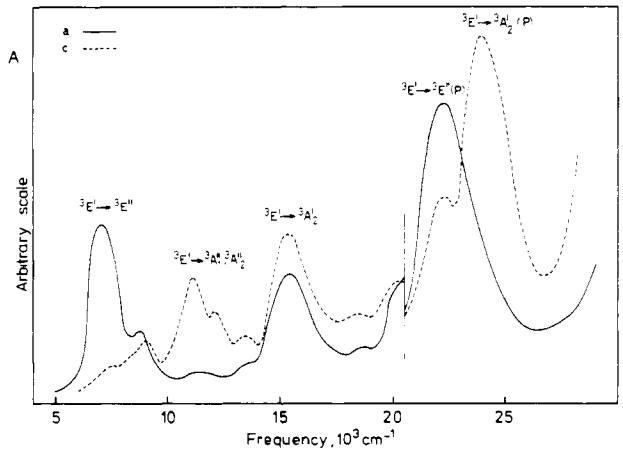

Figure 8. Single-crystal polarized electronic spectra of $[Ni_2(bdhe)_2](ClO_4)_2$ recorded at 4.2 K with the radiation incident on the (010) face: electric vector parallel to *a* (—) and parallel to *c* (---).

electronic structure of the host lattice. They were recorded with the radiation incident orthogonal to the (010) face, with the electric vector parallel to *a* and *c*. They are shown in Figure 8. The spectra are highly polarized and reveal a great number of bands. The spectra do not show appreciable variations from room temperature to 4.2 K. For the assignment it is useful to adopt the D_{3h} nomenclature, even if the symmetry of the complex is lower and the selection rules of that group are not obeyed. By comparison with similar chromophores,[23-26] the assignment shown in Table IV is suggested.

Discussion

The analysis of the magnetic properties of exchange-coupled metal ions can be made by using several different theoretical tools such as spin Hamiltonian formalism and valence bond, molecular orbital, and ligand field models. All of these have several advantages and disadvantages. However the simplest to be used and the most appropriate for ESR data is the spin Hamiltonian formalism, which allows one to relate the parameters observed for the couple to the parameters of the corresponding single ions. For the case of couples of different metal ions, a suitable spin Hamiltonian is shown in eq 1.

$$\mathcal{H} = \mu_B \mathbf{B}\cdot\mathbf{g}_1\cdot\mathbf{S}_1 + \mu_B \mathbf{B}\cdot\mathbf{g}_2\cdot\mathbf{S}_2 + \mathbf{S}_1\cdot\mathbf{D}_1\cdot\mathbf{S}_1 + \mathbf{S}_2\cdot\mathbf{D}_2\cdot\mathbf{S}_2 + J\mathbf{S}_1\cdot\mathbf{S}_2 + \mathbf{S}_1\cdot D\cdot\mathbf{S}_2 + \mathbf{d}\cdot\mathbf{S}_1 x \mathbf{S}_2 + \mathbf{I}_1\cdot\mathbf{A}_1\cdot\mathbf{S}_1 + \mathbf{I}_2\cdot\mathbf{A}_2\cdot\mathbf{S}_2 \quad (1)$$

The first terms of the spin Hamiltonian (eq 1) are the single ion Zeeman and zero field splitting terms, and the next three are the bilinear interaction terms, while the last two are the single ion hyperfine terms.

When J is the leading term in the spin Hamiltonian (eq 1), i.e., if it determines a large zero field splitting compared to that given by $\mathbf{D}_1$, $\mathbf{D}_2$, $\mathbf{D}$, or $\mathbf{d}$, only the total S values are good quantum numbers. With the Wigner–Eckart theorem it was shown[27] that the spin Hamiltonian parameters in the coupled representation are related to those of the single ions according to the relations in eq 2, where $\mathbf{g}_c$ and $\mathbf{D}_c$ are the spin Hamiltonian parameters for the couple, $\mathbf{A}_{c_1}$ and $\mathbf{A}_{c_2}$ are the hyperfine coupling constants of nucleus 1 and 2, respectively, in the couple, and

$$\mathbf{g}_c = c_1 g_1 + c_2 g_2 \qquad \mathbf{A}_{c_1} = c_1 A_1 \qquad \mathbf{A}_{c_2} = c_2 A_2$$
$$\mathbf{D}_c = D/2 - c_3 D/2 + c_3 D_1 - c_4 D/2 + c_4 D_2 \quad (2)$$

$$c_1 = [S(S+1) + S_1(S_1+1) - S_2(S_2+1)]/2S(S+1)$$
$$c_2 = [S(S+1) + S_2(S_2+1) - S_1(S_1+1)]/2S(S+1)$$
$$c_3 = [1/S(2S-1)]\{[3[S(S+1) + S_1(S_1+1) - S_2(S_2+1)]^2 - 4(S+1)^2 S_1(S_1+1)]/4(S+1)^2 + 3[(S+1)^2 - (S_1-S_2)^2][(S_1+S_2+1)^2 - (S+1)^2]/(4S+1)^2(2S+3)\}$$
$$c_4 = [1/S(2S-1)]\{[3[S(S+1) + S_2(S_2+1) - S_1(S_1+1)]^2 - 4(S+1)^2 S_2(S_2+1)]/4(S+1)^2 + 3[(S+1)^2 - (S_1-S_2)^2][(S_1+S_2+1)^2 - (S+1)^2]/(4S+1)^2(2S+3)\} \quad (3)$$

It must be stressed here that in the original derivation of these formulas no explicit mention to their limit of validity is given, although it is clear that they are correct only if the conditions mentioned above apply.

These formulas have been used sometimes for the interpretation of the spin Hamiltonian parameters of exchange-coupled pairs of dissimilar ions, although their validity has hardly been checked. Recently the ESR spectra of a copper(II)–manganese(II) pair in the lattice of dichloroaquo(pyridine *N*-oxide)copper(II) has been reported,[28] and the g values of the coupled $S = 2$ state have been found to be smaller than 2, a result which was felt to be surprising. Now the above system is especially well suited to check the validity of formulas 2 and 3, since the g and A values of the copper(II) single ion can be estimated by the values observed in the copper(II)–zinc(II) couple[29] and the g value of the manganese(II) ion can be safely assumed to be isotropic and equal to 2. Further the zero field splitting of the manganese(II) ion must be small, and the estimated separation of the $S = 3$ and $S = 2$ states is at least 250 cm^{-1}.[28]

For eq 3, with $S_1 = {}^1/_2$, $S_2 = {}^5/_2$, and $S = 2$, the g values in the coupled state are given by eq 4.

$$g_c = {}^7/_6 g_{Mn} - {}^1/_6 g_{Cu} \quad (4)$$

Equation 4 explains quite simply the g values smaller than the spin-only value. With the g_{Cu} values previously reported, the values $g_{cz} = 1.95$, $g_{cx} = 1.99$, and $g_{cy} = 1.99$ are obtained, in excellent agreement with the experimental data $g_1 = 1.952$, $g_2 = 1.991$, and $g_3 = 1.986$.

As far as the hyperfine interaction is concerned, the formulas in eq 3 demand that $\mathbf{A}_{Mn}$ in the couple is $7A_{Mn}/6$ of the single ion, while A_{Cu} is $-{}^1/_6$ that of the single ion. Since A in the copper(II)–zinc(II) pair was found to be 139×10^{-4} cm^{-1},[29] the agreement with the reported value[28] of 23×10^{-4} cm^{-1} is perfect. No data are available for the manganese(II)–zinc(II) pair, but the manganese(II) hyperfine coupling constant of 76×10^{-4} cm^{-1} reported for a MnO_2Cl_2 chromophore,[30] which is rather similar to the MnO_3Cl_2 one present in this complex, suggests a value of $A = 89 \times 10^{-4}$ cm^{-1} in the couple, again in excellent agreement with the value of 90×10^{-4} cm^{-1} reported for the copper(II)–manganese(II) couple.[29]

For the present $[M_2(bdhe)_2](ClO_4)_2$ complexes the situation does not seem to be so favorable. The symmetry of the complex is very low, and the zero field splitting of the nickel(II) and cobalt(II) ions in principle is not neglectable.[18] For the Ni–Cu couple we have $S_1 = {}^1/_2$, $S_2 = 1$, and $S = {}^3/_2$ and ${}^1/_2$. The g values for the $S = {}^1/_2$ state are related to those of the single ions according to eq 5.

$$g_c = {}^4/_3 g_{Ni} - {}^1/_3 g_{Cu} \quad (5)$$

(23) Ciampolini, M. *Struct. Bonding (Berlin)* **1969**, *6*, 52.
(24) Bertini, I.; Ciampolini, M.; Dapporto, P.; Gatteschi, D. *Inorg. Chem.* **1972**, *11*, 2254.
(25) Bertini, I.; Morassi, R.; Sacconi, L. *Coord. Chem. Rev.* **1973**, *11*, 343.
(26) Wood, J. *Prog. Inorg. Chem.* **1972**, *16*, 228.
(27) Chao, C. C. *J. Magn. Reson.* **1973**, *10*, 1.
(28) Krost, D. A.; McPherson, G. L. *J. Am. Chem. Soc.* **1978**, *100*, 987.
(29) After this manuscript was submitted, we became aware of a new paper by McPherson et al.[30] where the same conclusions are reached through a slightly different approach.
(30) Paulson, J. A.; Krost, D. A.; McPherson, G. L.; Rogus, R. D.; Atwood, J. L. *Inorg. Chem.*, in press.

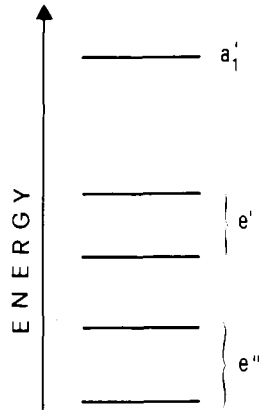

Figure 9. Energy level diagram for a monomeric unit possessing the geometrical features of $[Ni_2(bdhe)_2](ClO_4)_2$. The angular overlap parameters are $e_\sigma(O) = 3500$, $e_\sigma(Ni) = 4200$, $e_\sigma(N_2)(N_3) = 3700$, and $e_\pi = 0$ cm^{-1}.

For eq 5 to be used correctly the principal g directions of the single ions and of the pair should be known. The $g_\parallel$ of the pair is found to be very close to the "trigonal" axis of an idealized trigonal bipyramid. If the ESR spectra of the Zn–Cu complex are used as an estimate of the g values of the single copper(II) ion, it must be concluded that the unpaired electron is in an essentially d_{z^2} orbital, z being the trigonal axis. It seems reasonable therefore to assume that at least the g_z axis is the same for the single copper(II) ion and the Ni–Cu couple. With eq 5, the corresponding values of the nickel(II) single ion are calculated as $g_\parallel = 2.61$ and $g_\perp = 2.06$–2.09. These values should be compared to the average $g = 2.40$ calculated from the magnetic susceptibility data.[13]

In a perfect trigonal-bipyramidal environment the ground state of a nickel(II) ion should be $^3E'$,[23] and the g values for the ground doublet should be $g_\parallel = 8$ and $g_\perp = 0$.[25] However, in the present case the symmetry is far from D_{3h}, and it must be expected that the orbital degeneracy is removed. The single-crystal polarized electronic spectra of the pure $[Ni_2(bdhe)_2](ClO_4)_2$ complex show a marked splitting of the first band which should be attributed to the $^3E' \rightarrow {}^3E''$ transition in D_{3h} symmetry. Further the close similarity of the room temperature and 4 K spectra suggests that there are not levels appreciably populated at room temperature. Finally it must be mentioned that the selection rules do not conform to those of D_{3h} symmetry.

Sample calculations using the angular overlap model[31] suggest that the order of the levels for a MN_3O_2 chromophore, possessing the geometry of the present dimer, is as shown in Figure 9. The highest orbital can be described as essentially z^2 in nature, in agreement with the ESR data of the Cu–Zn complex, and the next two levels, which would be degenerate in pure D_{3h} symmetry and should correspond to xy and $x^2 - y^2$ orbitals, are largely split, confirming that the nickel(II) complex can be considered as orbitally nondegenerate.

The g values calculated above for the nickel ion show that a very large orbital contribution to the g value might be brought about by the near degeneracy of the ground level. However there is also the possibility that the g values suffer the influence of the zero field splitting of the nickel(II) ion. The complete Hamiltonian matrix for the $S_1 = {}^1/_2$, $S_2 = 1$ couple is given in Table V. The two blocks along the diagonal corresponding to the $S = {}^3/_2$ and $S = {}^1/_2$ states are in agreement with the eq 2 and 3. However, there are off-diagonal elements between $S = {}^1/_2$ and $S = {}^3/_2$ states involving the zero field splitting of the nickel(II) ion. It is easy to verify that the g values of the $S = {}^1/_2$ state are affected by the D_1 value. Therefore the estimated g values for the nickel(II) ion are affected by an error which depends on the J/D_1 ratio. The major conclusion which may be reached from the analysis of the ESR spectra of the Ni–Cu pair is that the coupling must be antiferromagnetic. This must be determined by the interaction of the z^2 orbitals, which, as shown by the data for the pure copper(II) dimer,[13] is antiferromagnetic, and that between the z^2 orbital of copper(II) and the xy (or $x^2 - y^2$) orbital of nickel(II). Since the latter are not in close contact, although orthogonal, they are not expected to give a large ferromagnetic interaction,[34] thus justifying the observed antiferromagnetism.

The ESR spectra of the Ni–Co couple are more puzzling. Since $S_1 = 1$ and $S_2 = {}^3/_2$, the possible S states are $S = {}^5/_2$, ${}^3/_2$, and ${}^1/_2$. The observed spectra appear to be due to transitions within one Kramers doublet, but this in principle might belong to each of the three S states. No other transition could be detected, leaving therefore the problem open about the state to which the Kramers doublet belongs. If the assumption is made that $JS_1 \cdot S_2$ is the leading term in the spin Hamiltonian, then either $S = {}^5/_2$ or $S = {}^1/_2$ can be the ground level. The effective g values do not conform to those usually found for a $S = {}^5/_2$ spin system split in zero field.[18,35] On the other hand the effective g values cannot be reconciled with a $S = {}^1/_2$ state. The g values for a trigonal-bipyramidal cobalt(II) complex must be close to 2,[36] since the ground state is $^4A_2$, i.e., orbitally nondegenerate. A support to this view comes also from the available ESR[18,37] and magnetic susceptibility data.[38] Even if the g values of the nickel(II) complex obtained above are used, it is not possible to justify the g values observed in the Ni–Co pair. On the other hand the observed g values also do not correspond to those expected for a $S = {}^3/_2$ system split largely at zero field,[18] ruling out the possibility of assigning the spectra to some high-spin cobalt(II) impurity. Also preliminary results on Co–Zn complex confirm that the g values of a single cobalt(II) ion are different.

It must be concluded that in this case the zero field splittings of both the ions are presumably large, and their effect may be that of making the order of the levels largely different from that predicted on the assumption of large J. Therefore for the Ni–Co pair it is not possible to obtain any meaningful information on the nature of the magnetic coupling on the basis only of these data.

Acknowledgment. Thanks are due to Professor L. Sacconi for encouragement. Thanks are also expressed to Dr. G. L. McPherson for making available to us his manuscript prior to publication.

Registry No. $[Ni_2(bdhe)_2](ClO_4)_2$, 23678-41-3; $[Cu_2(bdhe)_2](ClO_4)_2$, 73702-14-4; $[Co_2(bdhe)_2](ClO_4)_2$, 73702-12-2; $[Zn_2(bdhe)_2](ClO_4)_2$, 73702-16-6.

(31) Kokoszka, G. F.; Allen, H. C., Jr.; Gordon, G. *J. Chem. Phys.* **1967**, *46*, 3020.
(32) Vivien, D. G.; Gibson, J. F. *J. Chem. Soc., Faraday Trans.* **1975**, *71*, 1640.
(33) Schäffer, C. E. "Wave Mechanics"; Butterworths: London, 1972.
(34) Goodenough, J. "Magnetism and the Chemical Bond"; Interscience: New York, London, 1963.
(35) Aasa, R. *J. Chem. Phys.* **1970**, *6*, 326.
(36) Bencini, A.; Gatteschi, D. *J. Phys. Chem.* **1976**, *80*, 2126.
(37) Kennedy, F. S.; Hill, H. A. O.; Kaden, T. A.; Vallee, B. L. *Biochem. Biophys. Res. Commun.* **1972**, *6*, 1533.
(38) Duggan, D. M.; Hendrickson, D. N. *Inorg. Chem.* **1975**, *14*, 1944.